

Magnetoresistance of atomic-sized contacts: An *ab initio* study

A. Bagrets,^{1,2} N. Papanikolaou,³ and I. Mertig²

¹Max-Planck-Institut für Mikrostrukturphysik, D-06120 Halle, Germany

²Martin-Luther-Universität Halle, Fachbereich Physik, D-06099 Halle, Germany

³Institute of Microelectronics, NCSR "Demokritos," GR-15310 Athens, Greece

(Received 24 November 2003; revised manuscript received 26 February 2004; published 18 August 2004)

The magnetoresistance (MR) effect in metallic atomic-sized contacts is studied theoretically by means of first-principle electronic structure calculations. We consider three-atom chains formed from Co, Cu, Si, and Al atoms suspended between semi-infinite Co leads. We employ the screened Korringa-Kohn-Rostoker Green's function method for the electronic structure calculation and evaluate the conductance in the ballistic limit using the Landauer approach. The conductance through the constrictions reflects the spin-splitting of the Co bands and causes high MR ratios, up to 50%. The influence of the structural changes on the conductance is studied by considering different geometrical arrangements of atoms forming the chains. Our results show that the conductance through *s*-like states is robust against geometrical changes, whereas the transmission is strongly influenced by the atomic arrangement if *p* or *d* states contribute to the current.

DOI: 10.1103/PhysRevB.70.064410

PACS number(s): 73.63.Rt, 73.23.Ad, 75.47.Jn, 73.40.Cg

The investigation of electron transport through metallic atomic-sized contacts has attracted a lot of attention during the last 15 years, and most achievements are summarized in a recent review.¹ Using up-to-date experimental techniques, such as mechanically controllable break junctions² or scanning tunneling microscopy,^{3,4} it is possible to fabricate nanocontacts with a single atom, atomic chain, or a molecule⁵ in the constriction. The experiments reveal steplike changes of the conductance upon elongation of the nanocontacts.¹⁻⁴ In case of noble (Au, Ag, Cu)⁶⁻⁸ and alkali metals (Li, Na, K)⁷⁻⁹ conductance histograms show a dominant peak very close to one conductance quantum, $G_0=2e^2/h$, and smaller peaks close to integer conductance quanta. However, in case of transition metals the situation differs significantly^{8,10,11} and a broad distribution of conductance values is usually obtained.

To describe the nanocontacts theoretically, several methods have been developed by many groups during the last years. An approach based on the tight-binding (TB) Hamiltonian adapted for a nanocontact geometry was proposed in Refs. 12 and 13. An important conclusion of TB models is that the conductance of single-atom contacts is related to the number of valence orbitals of the contact atom available at the Fermi energy.^{12,14} Lang and coworkers¹⁵⁻¹⁸ and Kobayashi and coworkers^{19,20} studied the single-atom contacts,¹⁵ atomic chains of Al,^{16,19} Na,^{17,20} and C¹⁸ using *ab initio* calculations based on density functional (DF) theory with jellium electrodes. The formation mechanisms of atomic chains made from different types of elements such as Ni, Pd, Pt, Cu, Ag, and Au were investigated by means of molecular dynamics simulations.²¹ These studies were triggered by the experimental evidence of the formation of gold wires.⁴ Recently Mehrez *et al.*²² and Brandbyge *et al.*²³ presented fully self-consistent DF calculations of the conductance of atomic-sized contacts treating the electronic structure of both the contact and electrodes on the same footing.

In this paper, we present *ab initio* calculations of the conductance of nanocontacts and focus on magnetic systems. We consider magnetic semi-infinite fcc (001) Co electrodes

joined by nanocontacts of different materials. We assume that they take the form of short three-atom Co, Cu, Si, or Al chains suspended between the leads, as shown in Fig. 1. Our aim is to investigate whether such hybrid systems could exhibit a large magnetoresistance (MR) effect. We wish to address the following theoretical questions: (i) What is the influence of transition metal electrodes on the conductance of nanocontacts? (ii) What is the effect of the geometrical and electronic structure of the nanocontacts on the transport properties? (iii) What are favorable conditions to increase the MR through a constriction?

The structure of the nanocontacts studied below is presented in Fig. 1. The experimental lattice constant $a_0 = 6.70$ a.u. of fcc Co was used in the calculations. In the first configuration [Fig. 1(a)], we consider a linear three-atom chain with the first and the third atoms placed above the Co (001) surfaces at the ideal positions of the fcc structure with the distance to the middle-atom of the chain being $a_0/\sqrt{2}$, which is the nearest-neighbor distance in the fcc lattice. In the second (zigzag-like) configuration [Fig. 1(b)], the atomic chain is a continuation of the fcc structure along [001] direction, thus the symmetry is lower than in case of a linear chain. These two configurations were chosen to investigate

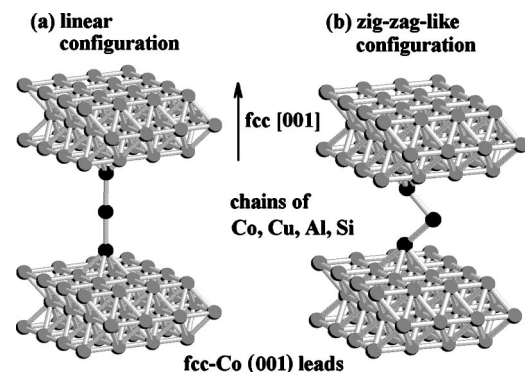


FIG. 1. Geometry of the nanocontacts: (a) linear configuration; (b) zigzag-like configuration.

TABLE I. Magnetic moments (μ_B) of atoms forming either linear or zigzag-like three-atom chains (see Fig. 1) for P and AP orientation of the magnetic moments in the Co leads. The “contact” atom of the chain sits above the (001) surface. The magnetic moment of bulk Co is $1.62 \mu_B$, the moment of the Co (001) surface atom is $1.78 \mu_B$.

Atoms	Co linear		Co zigzag		Cu linear		Cu zigzag		Al linear		Al zigzag		Si linear		Si zigzag	
	P	AP														
Contact	+1.91	+1.91	+2.00	+1.97	+0.08	+0.08	+0.08	+0.08	-0.09	-0.09	-0.10	-0.09	-0.11	-0.11	-0.07	-0.06
Central	+2.06	0.00	+2.28	0.00	+0.01	0.00	+0.03	0.00	0.00	0.00	0.00	0.00	+0.06	0.00	+0.11	0.00

the effect of the geometrical arrangement on the conductance.

The electronic structure was calculated using the nonrelativistic spin-polarized version of the screened Korringa-Kohn-Rostoker (KKR) Green’s function method (for details, see Ref. 24). The potentials were assumed to be spherically symmetric around each atom. However, the multipole expansion of the charge density was taken into account. The angular momentum cutoff for the wave functions and the Green’s function was chosen to be $l_{\max}=3$ to ensure well converged results. Within the KKR method,²⁴ the Green’s function of the systems is obtained in two steps. First, we calculate the Green’s function of the auxiliary system consisting of semi-infinite leads separated by a vacuum barrier. Next, the impurity problem is solved self-consistently by embedding the chain, surrounding atoms, and empty sites into the host system, in order to account for the charge and spin density redistribution effects. We assumed parallel (P) and antiparallel (AP) magnetic configuration for the Co leads. The electronic structure of the constriction was calculated self-consistently for both cases.

Ballistic conductance of the nanocontacts, g , was calculated using the Landauer theory as formulated by Baranger and Stone.²⁵ We consider two semi-infinite Co (001) bulk leads connected by the scattering region. Conductance is calculated between two atomic planes located in the ideal leads. We neglect tunneling current far away from the contact region and sum up current contributions in real space in the vicinity of the constriction. Convergence was checked in order to achieve errors less than 5% in the conductance evaluation. A detailed description and convergence properties of the method can be found in Ref. 26. The real-space version of the method employed here was also presented in Ref. 27.

In Table I, we present magnetic moments calculated for different atomic chains. We found that magnetic moment is enhanced for the Co atoms in the Co constriction reaching values up to $2.06 \mu_B$ for the central Co atom of the linear chain and $2.28 \mu_B$ for the zigzag geometry. In the AP configuration, due to symmetry, the central atoms of the chains have zero moments and the magnetic profiles are antisymmetric. In cases of Cu, Si, and Al, the induced magnetic moments are small, as can be seen from Table I.

Our results for the MR at the Fermi energy (E_F) are summarized in Table II. We define a MR ratio as $\text{MR}=(g_P - g_{AP})/g_{AP}$ where g_P , g_{AP} are the conductances for P and AP magnetic configurations, respectively, of the Co leads. The calculations predict a MR ratio of 30%–40% for the Co constriction, and of 20% in the case of the Cu chain suspended between the leads. The results for Al and Si chains are par-

ticularly interesting. We obtain a MR around 50% for the linear configuration although magnetic moments are rather small (see Table I). The values decrease to 20% when the symmetry of the constriction is reduced.

In order to understand the relation between electronic structure and transport properties, we consider the energy-dependent transmission $T(E)$ through the constriction (Figs. 2 and 3). In the linear response, the conductance per spin channel is related to the total transmission as $g = e^2/h \int_{-\infty}^{+\infty} \{-f'(E)\} T(E) dE$, where $f'(E)$ is the derivative of the Fermi-Dirac distribution function. For zero temperature, the conductance is $g = e^2/h T(E_F)$. However, in case of an applied voltage V , states in the energy window of eV close to E_F are relevant for the electron transport.

In Fig. 2, we present the transmission of Co, Cu, Al, and Si constrictions between Co leads for both spin channels for parallel magnetic configuration. We see that transmission for majority (spin-up) electrons is generally a rather smooth function of energy. However, for minority (spin-down) electrons, the transmission exhibits rather complicated behavior as a function of energy caused by Co d states, which also contribute to electron transport. In Fig. 3, we present the total transmission (sum of both spins), for parallel configuration in comparison with the antiparallel configuration. The conductance of the considered systems is the transmission at the Fermi energy $T(E_F)$, in units of e^2/h . The difference of the transmission between P and AP configurations at E_F is a measure of MR.

Let us first concentrate on Co constrictions [Figs. 2(a) and 2(b)]. The energy dependence of the transmission can be interpreted in terms of local densities of states (LDOS). For this reason, in Fig. 4, we present the symmetry projected LDOS, s , p , $d_{3z^2-r^2}$, d_{xz} , d_{yz} , at the Co central atom of the linear chain. In case of linear configuration the d_{xy} , $d_{x^2-y^2}$ orbitals do not support current since they are oriented perpendicular to the current direction (z axis) and form very sharp resonances in the LDOS of the central Co site of the chain because of weak coupling with the orbitals of the neighboring sites. From Fig. 4(a), we see that Co majority states close to E_F are mainly sp -like since the d band is fully

TABLE II. Magnetoresistance ratio $\text{MR}=(g_P - g_{AP})/g_{AP} \times 100\%$ for different zigzag and linear chains suspended between the Co leads.

	Co	Cu	Al	Si
Linear	29	16	49	50
Zigzag	38	18	19	21

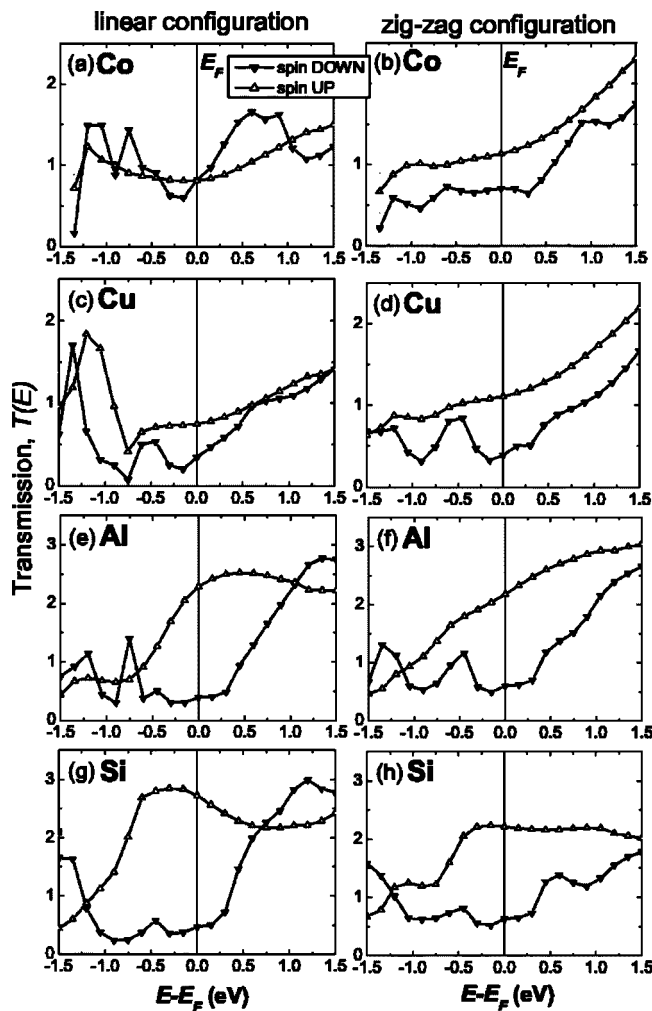


FIG. 2. Spin-dependent transmission as a function of energy for different linear (left column) and zigzag-like (right column) chains suspended between Co electrodes with magnetic moments oriented in parallel. The solid lines with up- and down-triangles correspond to transmission for spin-up and spin-down electrons, respectively.

occupied and located below -0.75 eV with respect to the Fermi energy, while for minority states the Fermi level crosses the d band. This is also valid for the case of a Co zigzag chain.

The examination of the LDOS at the Co sites of the linear chain shows that due to the localized and directional character of the d orbitals in real space, transmission is high only if the orbitals of the same symmetry at neighboring sites of the chain are coupled. This can be seen from Figs. 4(b) and 4(c). For example, the minority d_{xz} and d_{yz} states at -1.2 eV [Fig. 4(c)] survive also at the neighboring atom (dotted line) and cause high transmission. Similarly, the jump in the transmission around -0.75 eV for spin-down electrons [Fig. 2(a)] correlate with the peak of the minority $d_{3z^2-r^2}$ state [Fig. 4(b)].

Comparing Figs. 2(a) and 2(b), we can conclude that for Co constrictions the transmission of spin-up electrons is rather insensitive to structural changes simulated by the linear and zigzag configurations of the atomic chains. On the contrary, the geometrical arrangement of the constriction

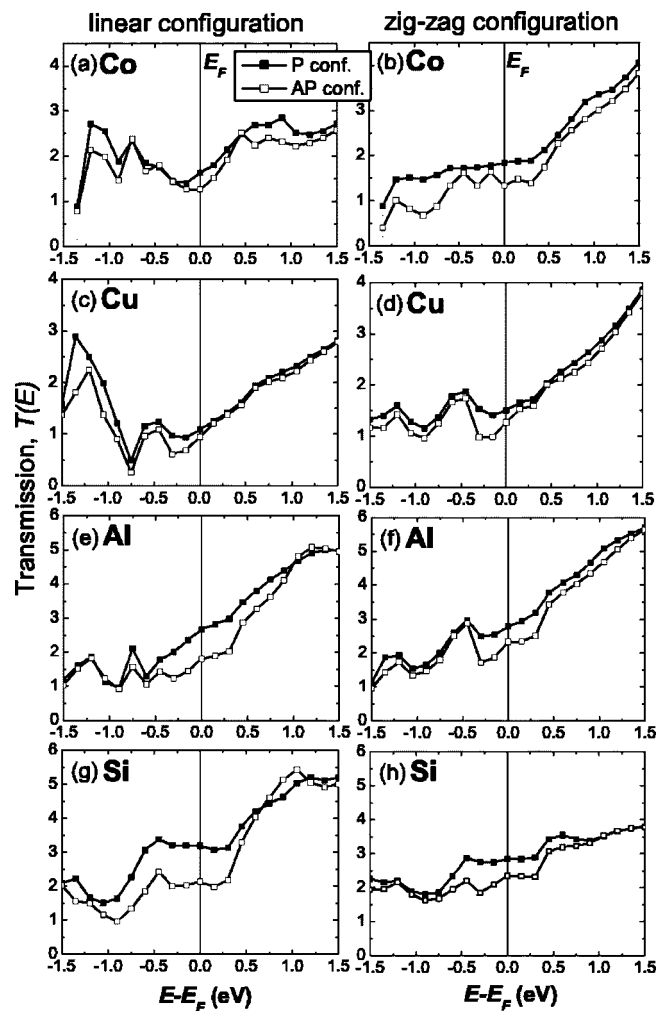


FIG. 3. Total transmission for both spins as a function of energy for different atomic chains suspended between the Co leads in case of parallel (black squares) and antiparallel (open squares) orientation of magnetic moments of Co. Transmission for the parallel configuration is the sum of the transmission for spin-up and spin-down electrons shown in Fig. 2. In case of the antiparallel configuration transmission is the same for both spins.

seems to be more important for d electrons. Reducing the symmetry of the atomic chain by considering zigzag geometry destroys coupling between d orbitals, therefore the transmission of spin-down electrons is reduced and we obtain a smooth energy dependence [see Fig. 2(b)].

Our study is restricted to collinear magnetic configurations. To estimate the influence of this approximation, we have considered also two-atom Co chains, where a 180° domain wall is formed in the antiparallel configuration. In that case MR at E_F was found to be approximately 15% and the overall behavior is not far from the one discussed above. Thus, our calculations predict a MR ratio rather sensitive to the geometrical and magnetic structure. In addition, the spherical potential approximation might lead to small shifts of the electronic states to different energies, compared to a more accurate full-potential description. This might influence the MR values at the Fermi level reported in the paper. In particular, in cases where there is a strong variation of the

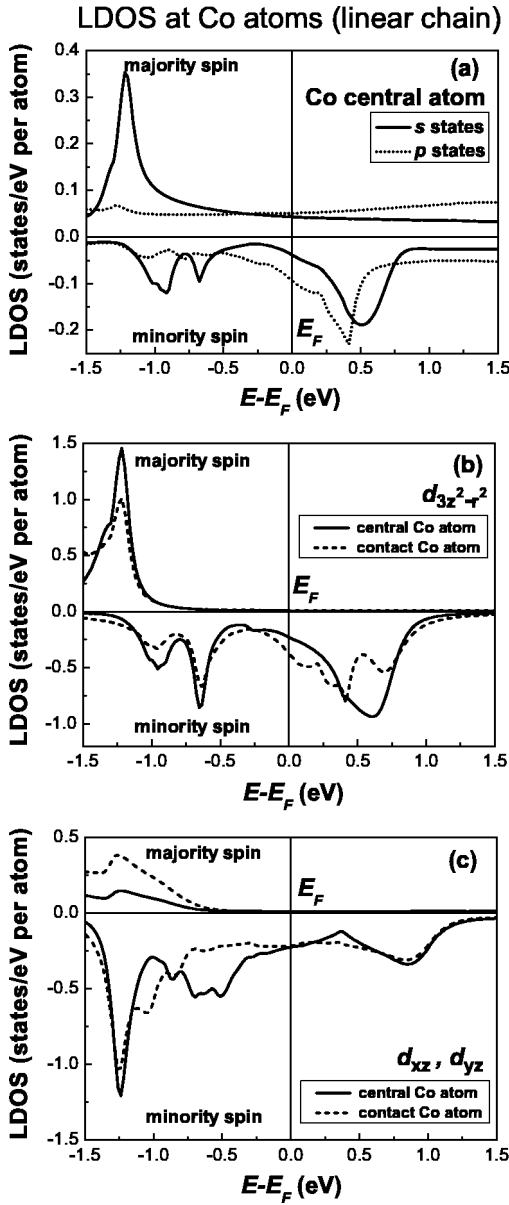


FIG. 4. Symmetry projected LDOS at the Co atoms of the linear three-atom chain for the case of parallel orientation of magnetizations in the Co leads. We present the s , p , and all d contributions relevant for a transport along the wire axis (z axis). The contact Co atom is the chain atom next to the surface of the Co lead. Panel (a): s and p states of the central Co atom; panel (b): $d_{3z^2-r^2}$ states of the central and contact Co atoms; panel (c): d_{xz} and d_{yz} states of the central and contact Co atoms.

transmission with energy close to the Fermi level, the reported MR values are expected to be less accurate. However, we believe that the configurations under consideration give a representative order of magnitude of the MR effect in Co nanocontacts, but cannot explain the MR ratio of Co contacts that was recently observed experimentally.²⁸ Moreover, our calculations for Ni nanocontacts using a zigzag configuration [Fig. 1(b)] give a MR value of 24%, contrary to the MR ratios of several hundreds percent observed in electrodeposited Ni nanocontacts.²⁸ Thus, our calculations show that within the accuracy of DF theory, the experimental values

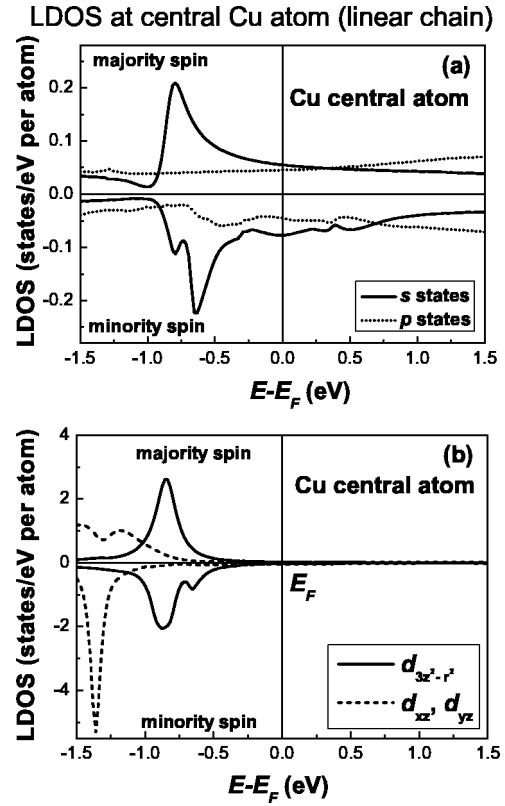


FIG. 5. Symmetry projected LDOS at the central Cu atom of the linear three-atom chain for the case of parallel orientation of magnetizations in the Co leads. Panel (a): s and p states; panel (b): $d_{3z^2-r^2}$, d_{xz} and d_{yz} states.

cannot be explained assuming a clean, abrupt domain wall and ballistic transport. Further investigations in particular on the role of defects on magnetotransport are required, since a recent study indicates a significant enhancement of the MR ratio if oxygen is assumed to be at the contact region.²⁹

The next question is whether the electronic structure of the leads affects the transport properties through constrictions? To answer this question the Co chains were replaced by Cu chains. It is well known that the majority band of Co matches the Cu band, whereas the minority band of Co differs strongly from the Cu band. Our results show that induced magnetic moments in the Cu chain are quite small (see Table I) and the spin-splitting of the LDOS is not significant (see Fig. 5). Consequently, the calculated difference of the transmission for the two spins is caused mainly by the Co leads [see Figs. 2(c) and 2(d)]. In case of the linear configuration, there are highly conducting states around -1.2 eV both for spin-up and spin-down channels. This is due to the matching of the Co d band to the Cu d states, which are located in the energy region below -0.75 eV [Fig. 5(b)]. However, these highly conducting channels are closed in the zigzag configuration [Fig. 2(d)] due to the same symmetry reasons discussed in case of the Co chains. Above -0.75 eV, the electronic structure of spin-up Co states and Cu states is similar, thus the majority (spin-up) transmission of the Cu chains [Figs. 2(c) and 2(d)] is similar to the majority transmission of the Co chains [Figs. 2(a) and 2(b)]. The energy-dependent transmission for spin-up electrons is smooth in

both configurations. However, the transmission of the spin-down electrons [Figs. 2(c) and 2(d)] is significantly reduced and, finally, a MR ratio of $\sim 15\%$ at E_F is obtained [see Figs. 3(c) and 3(d)]. The value $1.1 e^2/h$ of the majority (spin-up) conductance at E_F for three-atom zigzag chain of Cu is in agreement with the conductance of an infinite monoatomic zigzag chain of fcc Cu oriented along [001] direction. Since in that case only one band is crossing the Fermi level, the conductance is e^2/h per spin channel. Finally, we conclude that the electronic structure of the leads strongly influences the transmission through the constriction. The *s*-like states in the leads (majority states of Co) show a high transmission through an *s*-like chain; however, due to the band mismatch, *d*-like minority Co states are strongly scattered and show a low transmission through the Cu chain.

We further consider conductance through chains made from *sp* elements connected to the leads. We have chosen Si and Al, since Si clusters of 2–20 atoms can be produced in the gas phase;³⁰ thus measurements similar to Ref. 5 might be possible. Although the induced magnetic moments of Al and Si atoms are small, the MR ratio can be rather large (see Tables I and II). This is due to the “splitting” of the energy-dependent transmission curves, which reflects the spin-splitting of the Co bands [see Figs. 2(e)–2(h)]. For example, in case of a linear Si chain [Fig. 2(g)], the transmission of spin-up electrons increases up to 3 around -0.6 eV, while the spin-down channel has low transmission that rises only above E_F . As a consequence, the spin polarization of the current at E_F is high, $P=(g_{\uparrow}-g_{\downarrow})/(g_{\uparrow}+g_{\downarrow})=71\%$, which causes 50% MR [Figs. 3(g) and 3(h)]. The characteristic jump of ~ 2 in the transmission that is obtained in both spin channels at different energies can be explained by means of the spin-resolved LDOS at the Si sites (Fig. 6). The majority LDOS of the central atom shows a pronounced peak at -0.6 eV below E_F shaped like a van Hove singularity in a one-dimensional systems. This peak has p_x, p_y character. The same p_x, p_y peak is seen in the minority band, but it is shifted due to induced spin-splitting to higher energies just above E_F . This state is responsible for the increase of the transmission by ~ 2 . The minority LDOS of the central Si atom shows another pronounced resonance at -1.8 eV below E_F , which does not occur in the majority band and stems from the Co-Si interaction. This peak is also visible in the minority LDOS of the Si close to the Co surface. Since in the minority band the Si van-Hove-like state becomes unoccupied due to spin-splitting, the electrons occupy the state formed by the Co-Si interaction, which leads to nearly zero magnetic moments in the Si chain. The same effect of “splitting” of the energy-dependent transmission curves is also observed for Al, but the one-dimensional character of the

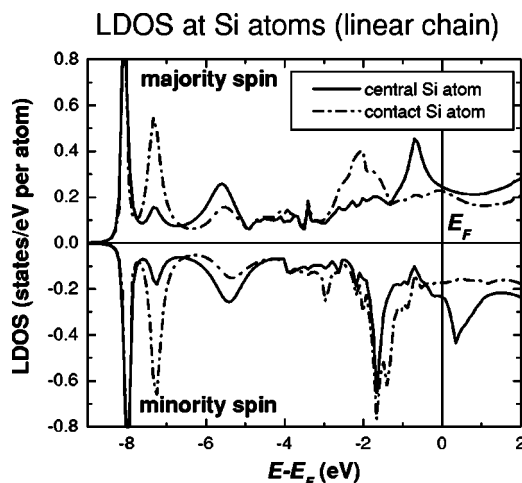


FIG. 6. Symmetry projected LDOS at the Si atoms of the linear Si chain in case of parallel orientation of magnetizations in the Co leads. Solid line: central Si atom; dashed-dotted line: contact Si atom next to the Co surface. The peaks of the LDOS around -1.8 eV and near E_F have p_x, p_y character.

p_x, p_y state is less pronounced compared to Si; therefore, the increase of the transmission of the linear Al chain is smoother [Fig. 2(e)].

In the zigzag configuration, the p_x, p_y degeneracy is lifted, so that for Si [Fig. 2(h)] the transmission increases in steps of ~ 1 both for spin-up and spin-down channels. In case of Al, the steps are not so pronounced [Fig. 2(f)]. Comparing the zigzag with the linear chains, we see that the splitting of the transmission curves is conserved in all cases [Figs. 2(e)–2(h)]. The MR ratio, however, drops for both Al and Si zigzag chains (Table II).

In conclusion, we have presented *ab initio* calculations of the conductance of magnetic atomic-sized contacts. MR ratios up to 50% are predicted for different three-atom chains suspended between Co leads. Our results show that the conductance through *s*-like states is robust against structural changes, whereas the transmission is strongly influenced by the atomic arrangement in the chain if *p* or *d* states contribute to the current. Furthermore, we have demonstrated that the spin polarization of the ferromagnetic leads induces a spin polarization of the current although the induced magnetic moments in the chain could be rather small (Cu, Al, Si). The induced spin-splitting of the wire states due to ferromagnetic leads is practically zero for *s* states, but could be as large as 1 eV for *p* states. In case of *sp* chains (Al, Si), this causes strong spin polarization of the current and, consequently, large MR values.

¹N. Agraït, A. Levy Yeyati, and J. M. van Ruitenbeek, Phys. Rep. **377**, 81 (2003).

²C. J. Muller, J. M. van Ruitenbeek, and L. J. de Jongh, Phys. Rev. Lett. **69**, 140 (1992); J. M. van Ruitenbeek,

Naturwissenschaften **88**, 59 (2001).

³G. Rubio, N. Agraït, and S. Vieira, Phys. Rev. Lett. **76**, 2302 (1996).

⁴H. Ohnishi, Yu. Kondo, and K. Takayanagi, Nature (London)

- 395**, 780 (1998); G. Rubio-Bollinger, S. R. Bahn, N. Agraït, K. W. Jacobsen, and S. Vieira, Phys. Rev. Lett. **87**, 026101 (2001).
- ⁵R. H. M. Smit, Y. Noat, C. Untiedt, N. D. Lang, M. C. van Hemert, and J. M. van Ruitenbeek, Nature (London) **419**, 906 (2002).
- ⁶M. Brandbyge, J. Schiøtz, M. R. Sørensen, P. Stoltze, K. W. Jacobsen, J. K. Nørskov, L. Olesen, E. Laegsgaard, I. Stensgaard, and F. Besenbacher, Phys. Rev. B **52**, 8499 (1995).
- ⁷J. M. Krans, J. M. van Ruitenbeek, V. V. Fisun, I. K. Yanson, and L. J. de Jongh, Nature (London) **375**, 767 (1995).
- ⁸B. Ludoph and J. M. van Ruitenbeek, Phys. Rev. B **61**, 2273 (2000).
- ⁹A. I. Yanson, I. K. Yanson, and J. M. van Ruitenbeek, Nature (London) **400**, 144 (1999); A. I. Yanson, Ph.D. thesis, Universiteit Leiden, The Netherlands, 2001.
- ¹⁰A. Enomoto, S. Kurokawa, and A. Sakai, Phys. Rev. B **65**, 125410 (2002).
- ¹¹H. E. van den Brom, A. I. Yanson, and J. M. van Ruitenbeek, Physica B **252**, 69 (1998).
- ¹²J. C. Cuevas, A. L. Yeyati, and A. Martín-Rodero, Phys. Rev. Lett. **80**, 1066 (1998).
- ¹³A. L. Yeyati, A. Martín-Rodero, and F. Flores, Phys. Rev. B **56**, 10 369 (1997); J. C. Cuevas, A. Levy Yeyati, A. Martín-Rodero, G. R. Bollinger, C. Untiedt, and N. Agraït, Phys. Rev. Lett. **81**, 2990 (1998); M. Brandbyge, N. Kobayashi, and M. Tsukada, Phys. Rev. B **60**, 17 064 (1999).
- ¹⁴E. Scheer, N. Agraït, J. C. Cuevas, A. Levy Yeyati, B. Ludoph, A. Martín-Rodero, G. Rubio Bollinger, J. M. van Ruitenbeek, and C. Urbina, Nature (London) **394**, 154 (1998).
- ¹⁵N. D. Lang, Phys. Rev. B **36**, 8173 (1987); **55**, 9364 (1997).
- ¹⁶N. D. Lang, Phys. Rev. B **52**, 5335 (1995).
- ¹⁷N. D. Lang, Phys. Rev. Lett. **79**, 1357 (1997).
- ¹⁸N. D. Lang and Ph. Avouris, Phys. Rev. Lett. **81**, 3515 (1998); **84**, 358 (2000).
- ¹⁹N. Kobayashi, M. Brandbyge, and M. Tsukada, Jpn. J. Appl. Phys. **38**, 336 (1999); N. Kobayashi, M. Aono, and M. Tsukada, Phys. Rev. B **64**, 121402 (2001).
- ²⁰N. Kobayashi, M. Brandbyge, and M. Tsukada, Phys. Rev. B **62**, 8430 (2000).
- ²¹S. R. Bahn and K. W. Jacobsen, Phys. Rev. Lett. **87**, 266101 (2001).
- ²²H. Mehrez, A. Wlasenko, B. Larade, J. Taylor, P. Grütter, and H. Guo, Phys. Rev. B **65**, 195419 (2002).
- ²³M. Brandbyge, J.-L. Mozos, P. Ordejón, J. Taylor, and K. Stokbro, Phys. Rev. B **65**, 165401 (2002).
- ²⁴N. Papanikolaou, R. Zeller, and P. H. Dederichs, J. Phys.: Condens. Matter **14**, 2799 (2002).
- ²⁵H. U. Baranger and A. D. Stone, Phys. Rev. B **40**, 8169 (1989).
- ²⁶Ph. Mavropoulos, N. Papanikolaou, and P. H. Dederichs, Phys. Rev. B **69**, 125104 (2004).
- ²⁷N. Papanikolaou, J. Opitz, P. Zahn, and I. Mertig, Phys. Rev. B **66**, 165441 (2002).
- ²⁸N. García, M. Muñoz, and Y.-W. Zhao, Phys. Rev. Lett. **82**, 2923 (1999); G. Tataru, Y.-W. Zhao, M. Muñoz, and N. García, *ibid.* **83**, 2030 (1999); N. García, M. Muñoz, G. G. Qian, H. Rohrer, I. G. Saveliev, and Y.-W. Zhao, Appl. Phys. Lett. **79**, 4550 (2001); H. D. Chopra and S. Z. Hua, Phys. Rev. B **66**, 020403 (2003).
- ²⁹N. Papanikolaou, J. Phys.: Condens. Matter **15**, 5049 (2003).
- ³⁰L. A. Bloomfield, R. R. Freeman, and W. L. Brown, Phys. Rev. Lett. **54**, 2246 (1985).